IEICE TRANS. ELECTRON., VOL. E84-C, NO. 12 DECEMBER 2001

PAPER Special Issue on New Technologies in Signal Processing for Electromagnetic-wave Sensing and Imaging

Polarimetric Correlation Coefficient Applied to Tree Classification

Makoto MURASE†, *Student Member,* Yoshio YAMAGUCHI†a), *and* Hiroyoshi YAMADA†, *Regular Members*

SUMMARY Tree canopies contain various scattering elements such as leaves, branches and trunks, which contribute to complex backscattering, depending on frequency and polarization. In this paper, we propose to use the polarimetric correlation coefficient for classifying trees, forests, and vegetations. The polarimetric correlation coefficient can be derived by the elements of Sinclair scattering matrix. Since the scattering matrix can be defined in any polarization basis, we examined the coefficient in the linear HV, circular LR, and optimum polarization bases. First, the change of correlation coefficient inside trees along the range direction is examined using small trees in a laboratory. The wider the range, the better the index. The coefficient defined in the LR polarization basis showed the largest change within tree canopy, which also contribute to retrieve scattering mechanism. Second, this index for discrimination is applied to polarimetric SAR data sets (San Francisco and Briatia area) acquired by AIRSAR and SIR-C/X-SAR. It is shown that polarimetric correlation coefficient in the LR basis best serves to distinguish tree types.

key words: *classification of target, tree canopy, Sinclair scattering matrix, polarimetric correlation coefficient*

1. Introduction

Radar polarimetry is now indispensable tool for monitoring earth cover. The advantage of using vector nature of electromagnetic wave is the information on the relations among polarimetric amplitudes and phases pertaining to target. Spaceborne and airborne polarimreic synthetic aperture radar (POL-SAR) system provide us with scattering matrix which may be related to biophysical and geophysical paramters on earth cover [1]–[5].

However, it is difficult to relate these radar data to actual situation or physical parameters correctly. For example, tree canopies contain various scattering elements such as leaves, branches, and trunks, which contribute to complex backscattering, depending on frequency and polarization [5], [6]. Therefore, even if we recoginize the data is derived from trees, there still remains a problem of what kind of trees are there. Is it conifer or broadleaf tree? Is it cedar or pine tree in conifer category? If we look into deeper, the interpretation of the radar data is quite difficult with respect to physical parameters. It is necessary to examine the fundamental scattering behavior to interpret remotely sensed data relating actual physical parameters or retrieve some useful indices for classifying targets.

Manuscript received March 26, 2001.
Manuscript revised June 18, 2001.

† The authors are with the Department of Information Engineering, Niigata University, Niigata-shi, 950-2181 Japan.
a) E-mail: yamaguch@ie.niigata-u.ac.jp

In this paper, we tried to retrieve useful index for classifying tree types between conifer and broadleaf trees. There would be several polarimetric indices such as entropy-$\bar{\alpha}$ angle [2], scattering matrix decomposition [5], correlation coefficient [6], and so on. Among them, entropy method did not provide a significant change (0.84 for conifer and 0.92 for broadleaf tree), and 3-component scattering decomposition could not discriminate these trees, because of highly complex scattering nature. Therefore the index employed here is the polarimetric correlation coefficient derived by the elements of Sinclair scattering matrix in the linear HV, circular LR, and the optimum polarization basis of a specific target. First, we introduce the polarimetric correlation coefficient in Sect. 2. Section 3 demonstrates the measured scattering matrix along the range direction. The change of correlation coefficient inside trees along the range direction is examined using small trees in a laboratory. The wider the range, the better the index. The coefficient defined in the LR polarization basis showed the largest change within tree canopy, which also contribute to retrieve scattering mechanism. In Sect. 4, this index for discrimination is applied to two polarimetric SAR data sets acquired by the NASA/JPL fully polarimetric AIRSAR system over San Francisco (Broadleaf tree area) and by SIR-C/X-SAR system over Briatia (Conifer area), in order to confirm the results. It is shown that polarimetric correlation coefficient in the LR basis best serves to distinguish tree types.

2. Radar Polarimetry

2.1 Scattering Matrix and Polarimetric Correlation Coefficient

Sinclair scattering matrix [$\boldsymbol{S}$] is defined in the polarization basis (HV) as,

$$\boldsymbol{E}_s = \begin{bmatrix} E_H^s \\ E_V^s \end{bmatrix} = \begin{bmatrix} S_{HH} & S_{HV} \\ S_{VH} & S_{VV} \end{bmatrix} \begin{bmatrix} E_H^t \\ E_V^t \end{bmatrix}$$

$$= \left[\boldsymbol{S}(HV) \right] \boldsymbol{E}_t \,, \qquad (1)$$

where $\boldsymbol{E}_t$ is the Jones vector of transmitted wave, and $\boldsymbol{E}_s$ is the scattered wave from target. The polarization basis is implied to be Horizontal (H) and Vertical (V) in this case. In the monostatic case, off-diagonal elements are equal, $S_{HV} = S_{VH}$, due to the reciprocity theorem. The scattering matrix can be considered as polarization transformer, specific to the target.

It is known in polarimetric data analysis and in polarimetric interferometry [5]–[7] that polarimetric correlation or coherence is effective for classifying targets. For distributed target such as forest or grass fields, many data tell us there is almost no coreelation between ensemble average of Co- and Cross-components, i.e., $\langle S_{HH} S_{HV}^* \rangle = \langle S_{VV} S_{HV}^* \rangle = 0$. Using the experimental results and the idea of polarimetric correlation with scattering matrix elements, we examined the following correlation coefficient in various polarization bases to classify tree types. In the HV basis case, the complex correlation coefficient between HH and VV channel can be constructed as,

$$\gamma_{HV} = |\gamma_{HV}| \angle \gamma_{HV} = \frac{\langle S_{HH} \cdot S_{VV}^* \rangle}{\sqrt{\langle |S_{HH}|^2 \rangle \langle |S_{VV}|^2 \rangle}}, \quad (2)$$

where $\langle \cdot \rangle$ is ensemble average.

The second candidate in the polarization basis is the circular polarization LR. This basis is effective for 3-component decomposition of scattering matrix [8], and provides useful classification scheme. Since the scattering matrix can be converted to that in any polarization basis, the expression in the LR basis becomes

$$\gamma_{LR} = |\gamma_{LR}| = \frac{\langle S_{LL} \cdot S_{RR}^* \rangle}{\sqrt{\langle |S_{LL}|^2 \rangle \langle |S_{RR}|^2 \rangle}} = \frac{\langle |\beta|^2 \rangle - \langle |\alpha|^2 \rangle}{\langle |\beta|^2 \rangle + \langle |\alpha|^2 \rangle} \quad (3)$$

where $\alpha = (S_{HH} - S_{VV})$ and $\beta = (2 S_{HV})$. If we assume trees area (forested field, vegetation field) showing reflection symmetry $\{\langle S_{HH} S_{HV}^* \rangle = \langle S_{VV} S_{HV}^* \rangle = 0\}$ [5], [7], α and β are found to be uncorrelated $\{\langle \alpha \beta^* \rangle = 0\}$. Under this assumption, the correlation coefficient γ_{LR} becomes real number. We will use absolute value of (3) for comparison with other coefficients.

The third candidate is the optimum polarization state basis [9] in the Co-Pol channel such that

$$\gamma_{OP} = |\gamma_{OP}| \angle \gamma_{OP} = \frac{\langle S_{AA} \cdot S_{BB}^* \rangle}{\sqrt{\langle |S_{AA}|^2 \rangle \langle |S_{BB}|^2 \rangle}}, \quad (4)$$

where, S_{AA} and S_{BB} are the elements of scattering matrix in diagonalized form [9].

$$S_{AA} = \frac{e^{j\phi_1}}{1 + \rho\rho^*} \left(S_{HH} + 2\rho S_{HV} + \rho^2 S_{VV} \right), \quad (5a)$$

$$S_{BB} = \frac{e^{j\phi_2}}{1 + \rho\rho^*} \left(\rho^{*2} S_{HH} - 2\rho^* S_{HV} + S_{VV} \right). \quad (5b)$$

The above expressions are derived by Co-Pol Max polarization state, corresponding to the polarization ratio ρ as

$$\rho_{cm1,2} = \frac{-B \pm \sqrt{B^2 - 4AC}}{2A}, \quad (6)$$

where, $A = S_{HH}^* S_{HV} + S_{HV}^* S_{VV}$, $B = |S_{HH}|^2 - |S_{VV}|^2$ and $C = -A^*$.

This optimum state applies only to a specific scattering matrix (or specific representative scattering matrix) in SAR image. Therefore, we take this polarization basis after determining the desired target's scattering matrix.

2.2 Polarization Signature

If scattering matrix [S] has been measured, it is possible to synthesize the radar channel power at any polarization state. For the Co-pol channel case, the received power is obtained from

$$P_C = \left| \boldsymbol{E}_t^T \left[\boldsymbol{S}(HV) \right] \boldsymbol{E}_t \right|^2. \quad (7)$$

The superscript T denote trnanspose. The variation of the received power with respect to the transmitting polarization state illustrates the polarimetric scattering behavior of a target [13] . This is called polarization signature and is an useful visual-aid for identifying target. The polarization signature is illustrated as a power pattern as a function of ellipticity angle and tilt angle of transmitting polarization [13].

3. Laboratory Experiment

In order to check the difference in polarimetric response of trees, conifer (needle-like leaf) and broadleaf tree were chosen as radar target in anechoic chamber as shown in Fig. 1. These trees are decorative plants with hight more than 50 cm. The maximum horizontal width of canopy is 30 cm.

The experimental situation is illustrated in Fig. 2. The polarimetric measurement specification are listed in Table 1, where H stands for horizontal and V for vertical. The radar antennas used are standard rectangular horns with aperture size of 10.8 cm by 8.0 cm, so that the beam width is approximately $19^\circ \times 19^\circ$ in the E- and H-plane. Their center positions are seperated by 16 cm for HH and VV cases and 11.5 cm for HV as configuration shown in Fig. 3. Although the radar system is slightly bistatic, this seperation is the minimum attainable distance for physical configuration. This slightly bistatic system can be calibrated to be monostatic system by the polarimetric calibration [10]. A set of 4 antennas were scanned in the horizontal direction. The radar wave implinges horizontally in this measurement so that 2-dimensional high resoultion imaging across trees becomes available. The measurement system is based on a network analyzer (HP8720C) in a stepped-frequency mode. The frequency bandwidth is from 9.0 to 11.0 GHz, (a total of 401 frequency

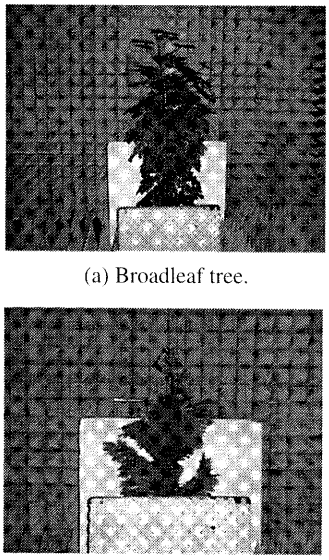

(a) Broadleaf tree.

(b) Conifer.

Fig. 1 Photographs of trees used in experiment.

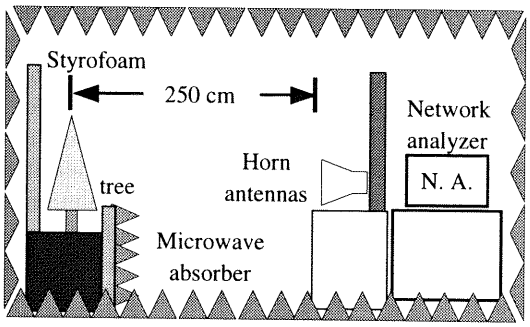

Fig. 2 Imaging geometry of a small tree.

Table 1 Measurement specification.

System	Network analyser (HP8720C)
Antennas	Rectangular horn
Polarizations	HH, HV, VV
Frequency points	401 points
Sweep frequency range	9.0 - 11.0 GHz
Scanning interval	1.0 cm
Scanning area	32 cm

points). This X-band was chosen just for a reason of our equipment restriction, although the L- or C-band system might be suitable for tree classification. We tried to achieve scale model as much as possible using small leaf trees so that the experimental results hold for other bands (except for dielectric property).

First, an empty room was measured to remove environmental reflections and antenna coupling. After the polarimetric calibration [10] and synthetic aperture processing [11], the experimental scattering matrix was obtained. Since range resolution $\Delta R = \frac{c}{2B}$ can be chosen arbitrary by choosing the bandwidth B of transmitting signal, we used B

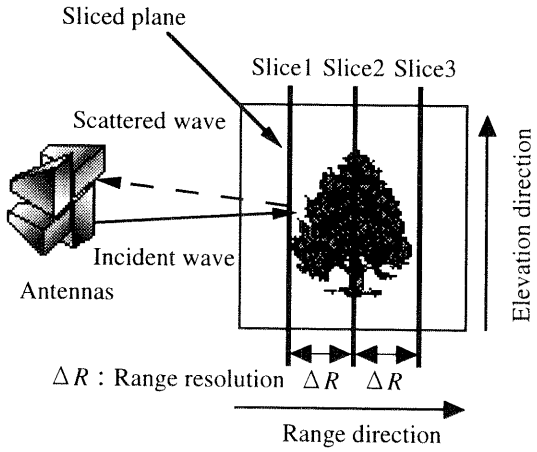

Fig. 3 Geometry of sliced plane along range direction.

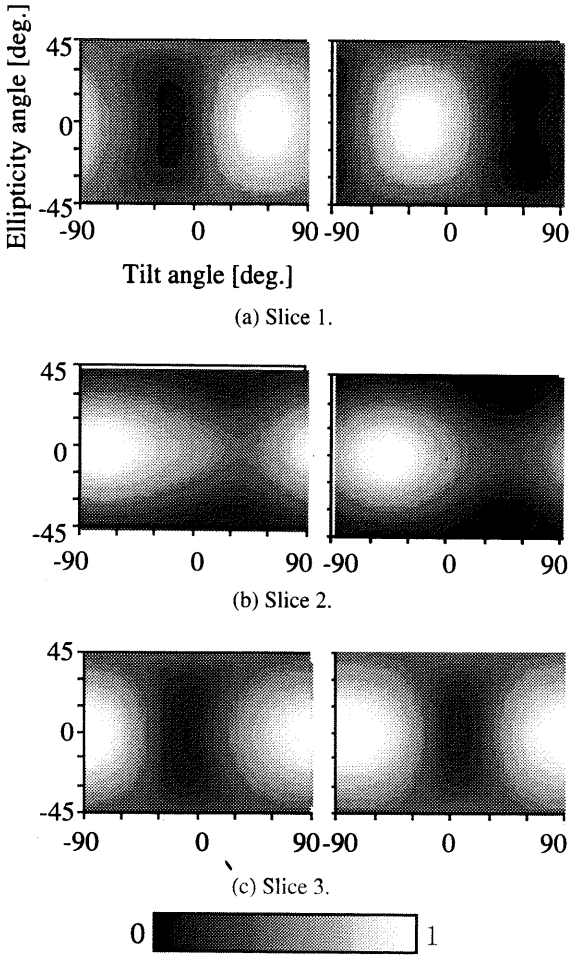

Fig. 4 Polarization signature at sliced planes Broaleaf tree (left), Conifer (right).

= 2 GHz as mentioned above. This bandwidth results in the range resolution of 7.5 cm, which covers the entire range of tree canopy width [12]. This benefits us to retrieve scattering mechanism within the canopy. Therefore, it is possible to check the polarimetric information at sliced planes as shown in Fig.

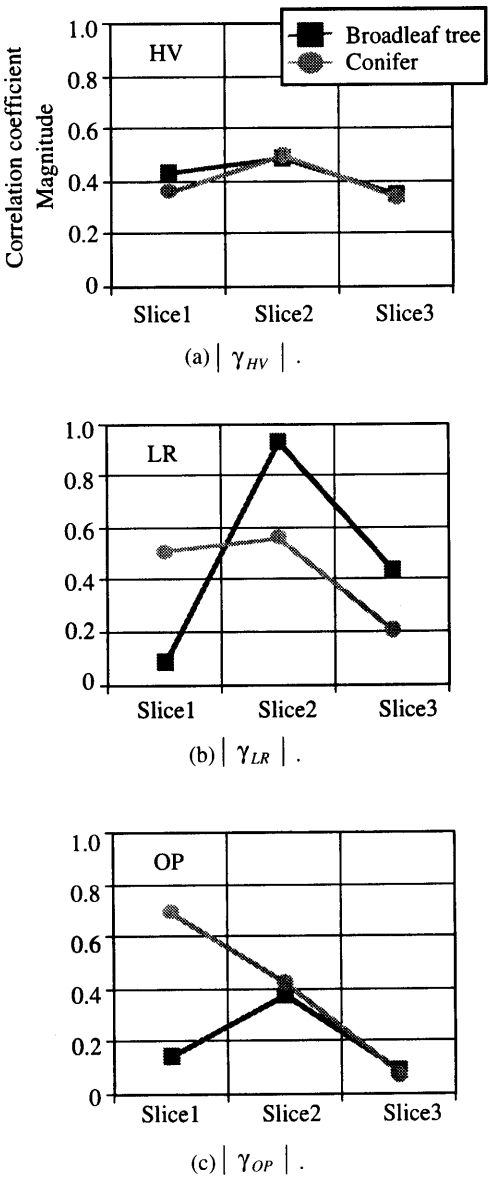

Fig. 5 Magnitude of correlation coefficient of slice plane along range direction.

3, where slice 2 is located at the center of tree trunk and 250 cm apart from the radar antenna.

The polarization signatures of trees at sliced planes 1–3 are shown in Fig. 4. The left side is for broadleaf tree and the right side is for conifer. These polarization signatures at slice 1 plane in Figs. 4 (a) and (c) are similar to those of oriented wires [10]. Then at slice 2 in Fig. 4 (b) the power becomes broaden at linear polarization states. On the other hand, the power becomes small at the circular polarization states. As the radar wave penetrates into deeper at slice 3, these signature shapes become similar to those of mixture of plate and wire plus pedestal (incoherent power) [13]. These results in Fig. 4 indicate multiple scattering occurs as we look deeper within the canopy. The broading peak phenomenon is more significant in conifer.

The magnitude of correlation coefficients for these trees are shown in Fig. 5. The correlation coefficient in the HV basis does not provide the difference of trees at all. The magnitude is approximately 0.4 throughout the canopy. The value is not so high. For correlation in the LR basis, it shows a significant change in the canopy, depending on the position. At slice 2 where tree trunk exists, the value attains the highest, 0.9, for broadleaf tree. For the optimum polarization basis (for scattering matrix at slice 1), the value is quite different for conifer and broaleaf tree. However, the value coincide with each other within the canopy. This fact tells that forefront scattering matrix is sensistive to the orientation and shape of target in that position. If range resolution is fine compared to target extension, the forefront information plays essential polarimetric response. Judging from the results, the correlation coefficient in the LR basis may serve to distiguish tree types.

4. POL-SAR Validation

In order to check the applicability of correlation coefficient to classify tree types, we analyzed actual POL-SAR data. Figure 6 shows the L-band images of San Francisco (Broadleaf area) obtained by AIRSAR and Briatia (Conifer area) by SIR-C / X-SAR. Although the frequency band is different

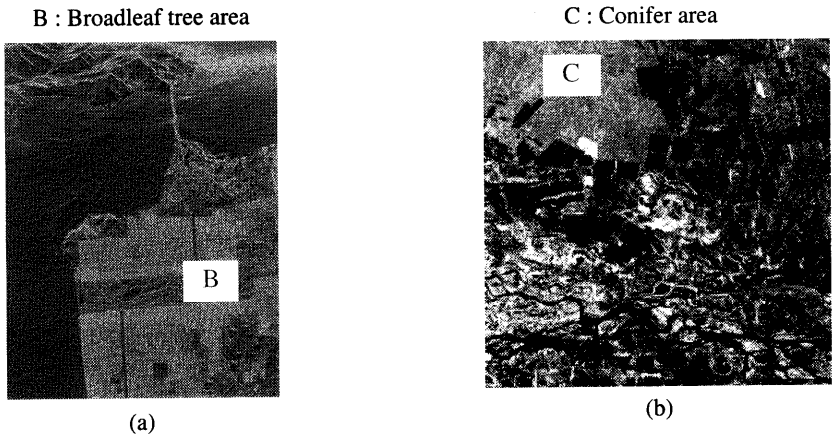

Fig. 6 L-band POL-SAR Total power image. (a) San Francisco, (b) Briatia.

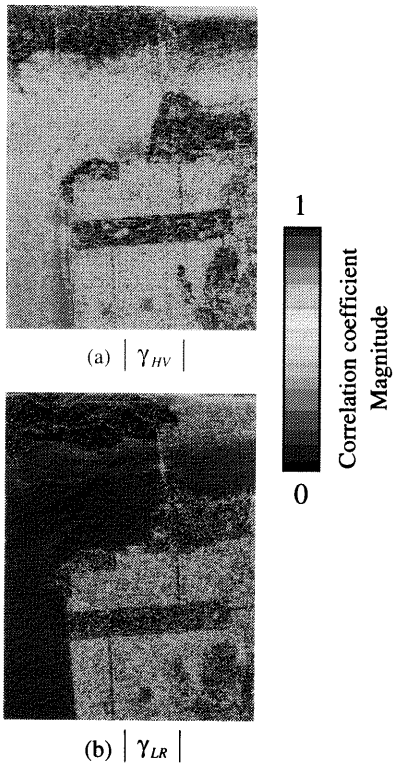

Fig. 7 $|\gamma_{HV}|$, $|\gamma_{LR}|$ images (San Francisco).

from X band, we expect to see the characteristics mentioned in the previous section.

Figure 7 also shows corresponding $|\gamma_{HV}|$ and $|\gamma_{LR}|$ map of San Francisco. It is seen that ocean area in Fig. 7(a) is fairly strong in comparison to that in Fig. 7(b).

First, we picked up 3 areas (area1, area2, area3) within the subarea B denoted in Fig. 6(a) and also 3 within C in Fig.

Table 2 San Francisco (Broadleaf tree area).

	$\lvert\gamma_{HV}\rvert$	$\lvert\gamma_{LR}\rvert$	$\lvert\gamma_{OP}\rvert$
area1	0.176	0.384	0.457
area2	0.189	0.342	0.370
area3	0.211	0.261	0.290

Table 3 Briatia (Conifer area).

	$\lvert\gamma_{HV}\rvert$	$\lvert\gamma_{LR}\rvert$	$\lvert\gamma_{OP}\rvert$
area1	0.154	0.583	0.560
area2	0.177	0.664	0.627
area3	0.098	0.750	0.668

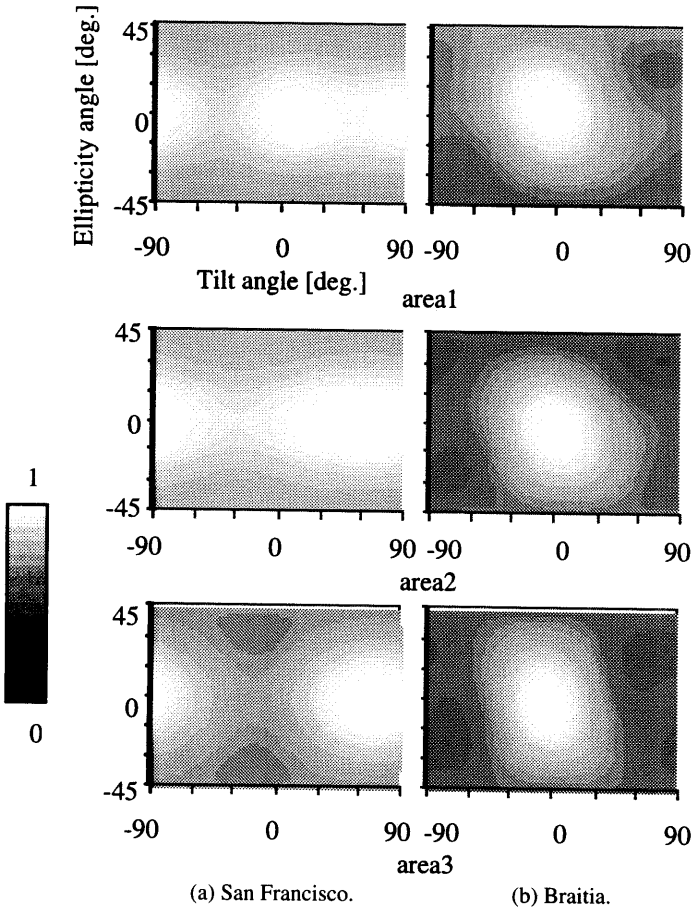

(a) San Francisco. (b) Braitia.

Fig. 8 Polarization signatures of tree area.

6(b). These areas are covered with trees and their size is approximately 38 m by 38 m (containing 3 by 3 pixels each). We calculated the polarimetric signature for these 3 areas. It is seen in Fig. 8(a) that polarimetric signatures appear to be composed of a variable portion sitting on a pedestal [13]. In Fig. 8(b), tree scattering is consistent with that predicated by slightly rough surface scattering. Second, we calculated the polarimetric correlation coefficient. The results are listed in Tables 2 and 3. It is seen that the results of $|\gamma_{LR}|$ is much more dependent on tree types than $|\gamma_{HV}|$. The value of $|\gamma_{LR}|$ is 0.26 – 0.38 for broadleaf trees and 0.58 – 0.75 for conifer in actual data. This fact also supports the superiority of $|\gamma_{LR}|$ for classification of trees.

5. Conclusion

Among many polarimetric parameters to describe target characteristics, the proposed polarimetric correlation coefficient defined in the circular polarization basis seems good index for discriminating conifer and broadleaf tree. This fact was confirmed in a laboratory measurement and by actual POLSAR images. Therefore, classification algorithm with the $|\gamma_{LR}|$ will enhance ability for discrimination and classification of tree type.

Acknowledgement

This work in part was supported by Grant in Aid for Scientific Research, Ministry of Education, Japan. Authors are grateful to NASA JPL for providing the fully polarimetric data.

References

[1] D.L. Evans, T.G. Farr, J.J. Van Zyl, and H.A. Zebker, "Radar polarimetry: Analysis tools and applications," IEEE Trans. Geosci. Remote Sensing, vol.26, no.6, pp.774-789, Nov. 1988.
[2] S.R. Cloude and E. Pottier, "An entropy based classification scheme for land applications of polarimetric SAR," IEEE Trans. Geosci. Remote Sensing, vol.35, no.1, pp.68-78, Jan. 1997.
[3] H. Hirosawa, Y. Matuzaka, M. Daito, and H. Nakamura, "Measurement of a backscatter from a cypress with and without leaves," IEEE Trans. Geosci. Remote Sensing, vol.27, no.6, pp.698- 701, Nov. 1989.
[4] S.R. Cloude, J. Fortuny, J.M. Lopez-Sancdez, and A.J. Sieber, "Wide-band polarimetric radar inversion studies for vegetation layers," IEEE Trans. Geosci. Remote Sensing, vol.37, no.5, pp.2430-2441, Sept. 1999.
[5] Proc. 4th Int. Workshop Radar Polarimetry, IRESTE, Nants, France, July 1998.
[6] S.V. Nghiem, S.H. Yueh, R. Kwok, and F.K. Li, "Symmetry properties in polarimetric remote sensing," Radio Science, vol.27, pp.693-711, Sept. 1992.
[7] S.R. Cloude and K.P. Papathanassiou, "Polarimetric SAR interferometry," IEEE Trans. Geosci. Remote Sensing, vol.36, pp.1551-1565, no.5, Sept. 1998.
[8] E. Krogager and Z.H. Czyz, "Properties of the sphere, diplane, helix decomposition," Proc. 3rd Int. Workshop Radar Polarimetry, vol.1, pp.106-114, March 1995.
[9] W.-M. Boerner, W.-L. Yan, A.-Q. Xi, and Y. Yamaguchi, "On the basic principles of radar polarimetry: The target characteristic polarization state theory of Kennaugh, Huynen's polarization fork concept, and its extension to the partially polarized case," Proc. IEEE, Special Issue on Electromagnetic Theory, vol.79, pp.1538-1550, Oct. 1991.
[10] K. Kitayama, Y. Takayanagi, Y. Yamaguchi, and H. Yamada, "Polarimetric calibration using a corrugated parallel plate target," IEICE Trans., vol.J81-B-II, no.10, pp.914-921, Oct. 1998.
[11] Y. Yamaguchi, Fudamentals of polarimetric radar and its applications, pp.63-74, Realize Inc., 1998.
[12] M. Murase, Y. Yamaguchi, and H. Yamada, "X-band polarimetric synthetic aperture radar imaging of a small tree," Proc. ISAP 2000, vol.3, pp.1255-1258, Aug. 2000.
[13] J.J. van Zyl, H.A. Zebker, and C. Elachi, "Imaging radar polarization signatures: Theory and observation," Radio Science, vol.22, pp.529-543, 1987.

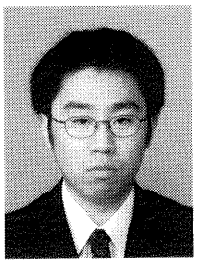

Makoto Murase was born in Gifu, Japan, on January 25, 1977. He received the B.E. and M.E. degrees from Niigata University, Niigata, Japan, in 1999 and 2001, respectively. He was engaged in SAR image analysis and target classification using radar polarimetry.

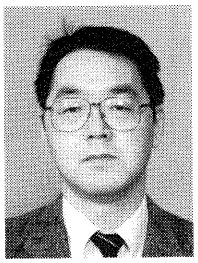

Yoshio Yamaguchi received the B.E. degree in electronics engineering from Niigata University in 1976, and the M.E. and Dr. Eng. degrees from Tokyo Institute Technology in 1978 and 1983, respectively. In 1978, he joined the Faculty of Engineering, Niigata University, where he is a professor. From 1988 to 1989, he was a Research Associate at the University of Illinois, Chicago. His interests are in the field of propagation characteristics of electromagnetic waves in lossy medium, radar polarimetry, microwave remote sensing and imaging. Dr. Yamaguchi is a senior member of IEEE, and a member of the Japan Society for Snow Engineering.

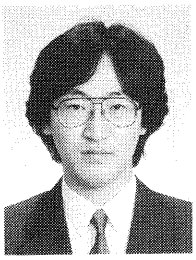

Hiroyoshi Yamada was born in Hokkaido, Japan, on November 2, 1965. He received the B.S., M.S., and Ph.D. degrees from Hokkaido University, Sapporo, Japan, in 1988, 1990, and 1993, respectively, all in electronic engineering. Since 1993, he has been with Niigata University, where he is an associate professor. His current research involves superresolution techniques, time-frequency analysis, electromagnetic wave measurements, and radar signal processing. Dr. Yamada is a member of IEEE.